Reprint from

T. Ishiguro K. Kajimura (Eds.)

Advances in Superconductivity II

Proceedings of the 2nd International Symposium on Superconductivity (ISS '89), November 14–17, 1989, Tsukuba

---

Springer-Verlag
Tokyo Berlin Heidelberg New York
London Paris Hong Kong

Direct Observation of Superconducting Magnetic Fluxons Using Electron Holography

S. HASEGAWA[1], T. MATSUDA[1], J. ENDO[1], A. TONOMURA[1], and R. AOKI[2]

[1] Advanced Research Laboratory, Hitachi, Ltd., Kokubunji, Tokyo, 185 Japan
[2] Faculty of Engineering, Osaka University Suita, Osaka, 565 Japan

ABSTRACT

The magnetic flux lines of a quantized flux (fluxon) penetrating through a superconducting Pb film were observed directly and individually by the electron holography technique using the Aharonov-Bohm effect. The digital phase analysis at the optical reconstruction stage in electron holography confirms the quantized flux value h/2e, and has potentiality to analyze the fluxon core structre in detail.

KEY WORDS: fluxon, flux line lattice, electron holography
fringe scanning interferometry, Aharonov-Bohm effect

INTRODUCTION

The essential nature of superconductivity has been unveiled through its peculiar magnetic behaviors, the Meissner effect, flux quantization, flux line lattice structures, and so on. They were phenomenologically understood by the Ginzburg-Landau theory, and recognized to be closely related to the fundamental of superconductivity through the Gor'kov theory besed on the BCS theory.

Although a great amount of efforts have been made to clarify the high-T_c superconducting mechanism since its discovery, we have not yet reached a consistent understanding. As in the case of low T_c superconductivity, important information on the high T_c superconducting mechanism is expected to be brought through their magnetic structure analysis.

Dynamical behaviors of fluxons also play an important role in the transport characteristics, limitting the critical current. Especially in the high T_c superconductors, the flux creep, flux line lattice melting, and fluxon-antifluxon pairs are expected to dominatly affect the transport characteristics.

Electron holography, invented by D. Gabor to improve the resolution of electron microscopes, has been realized with an electron microscope equipped with a cold field emission electron gun, which produces highly coherent electron beams, and an electron biprism. Its new applications have been developed, direct observation of magnetic field with high spatial resolution. Magnetic field can be revealed in the form of magneic flux line distribution[1]. We have successfully employed the electron holography technique for the direct observation of superconducting magnetic fluxons. Although this technique has a potentiality of dynamical observation of fluxons, we focus ourselves here on the static observation.

OBSERVATION OF MAGNETIC STRUCTURES IN SUPERCONDUCTORS

Various kinds of experimental techniques have been employed to investigate the magnetic structures in superconductors[2]. We summarize them based on their spatial resolution and the sensitivity for magnetic flux. Figure 1 shows rough estimates of availability of typical experimental methods.

The shadowed area covers the resolution and sensitivity necessary for observing the mixed state in type II superconductors. The Bitter method has been most widely used, including its recent applications to high T_c superconductors[3], only for qualitative discussions. The neutron diffraction method allows the very quantitative analysis on the flux structures, only when the flux is periodically distributed . Recent observations using scanning tunneling microscopy reveal a flux line lattice[4], which, however, does not probe the magnetic flux itself, but the electronic structure surrounding the fluxon at the surface. Electron holography enables one to directly observe the fluxons very quantitatively with high spatial resolution and analyze the individual fluxon core structure, even when the flux is not periodically distributed[5].

ELECTRON HOLOGRAPHIC OBSERVATION

The principle underlying the electron holographic observation of magnetic flux is the Aharonov-Bohm effect[6]. It predicts that the magnetic flux Φ causes the phase shift $\Delta\phi$ beween the electron waves passing through the different sides of the flux (Fig. 2):

$$\Delta\phi = 2\pi\frac{\Phi}{(h/e)}$$

A single flux quantum h/2e, therefore, causes the phase shift of π. Electron holography makes it possible to explicitly measure the phase of electron wave. When we draw the contour phase lines (the interference fringes) at a phase interval of π, they directly correspond to the magnetic flux lines in units of h/2e.

Our superconducting films were prepared by vacuum evaporation of Pb on one side of a tungsten wire of 30 μm-diameter. The critical temperature of the Pb film was 7.2 K and the residual resistance ratio between T=300K and 7.5K was 50~80. The film was cooled down to 4.5K to be superconducting with fluxons under a transverse magentic field of 3G in our holography electron microscope (Fig. 3). We can regard the illuminating electron wave as a plane wave. Transmitting through the sample region, the wavefront is deformed by the magnetic field; the localized field of a fluxon causes abrupt phase change, although the wavefront passing far from the Pb film is inclined smoothly because of a uniform field. By electron biprism action, the transmitted wave is devided into two parts, superimposed, and interfered to each other. Interference fringe is recorded on a hologram.

After developing and fixing the hologram, it was set in a laser interferometer (Fig. 4). The He-Ne laser beam is devided into two beams, and each irradiates the hologram with a different angle. A set of the $\pm$first-order diffracted waves emerges for each illuminating beam. Only the first-order diffracted wave from one beam and the $-$first-order one from the other beam are selected, and are made interfere with each other to form a interference micrograph. The interference fringes in this image are contour phase lines of π interval, which correspond to the magentic flux lines in units of a single fluxon.

Figure 5 shows the interference micrographs thus obtained. The lower black parts are the films and the upper, vacuum. The fringes show magnetic flux lines that fan out into free space after penetrating through the superconductor. In the case of Pb film of 1.0 μm thickness, the penetrating flux is a bundle of several fluxons, which is the type-I behavior. When the film thickness decreases, 0.2 μm, the flux becomes a single fluxon, the type-II behavior. We also observed fluxon-antifluxon pairs. They may have been created when the film was cooled through the Kosterlitz-Thouless regime, just below the T_c[7], and pinned so that the opposite fluxons would have not met to annihilate each other. The polarity of the flux cannot be distinguished with any other methods but electron holography.

The electron wavefront itself can be reconstructed from the hologram using "fringe scanning interferometry"[8]. Stepwise movement of the mirror A in Fig. 4, driven by a piezoelectric transducer(PZT), causes a fringe shift in the ineterference micrograph. Images at four different mirror positions, of which position interval is $\lambda/8$ (λ is the wavelength of the laser beam), were synchronously stored through a TV camera in a computer. The phase value at each pixel on the image was calculated from the brightness values at the corresponding pixel in the four images, and the original electron wavefront is numerically reconstructed.

The wavefront reconstructed from the hologram of 1.0 μm Pb film (Fig. 5(a)) is 3-dimensionally shown in Fig. 6, which is an expected one in Fig. 3. The abrupt phase shifts at the flux exits on the surface are multiples of π, and their multiples are the number of fringes in Fig. 5(a). This precisely means the flux quantization in units of h/2e. From the curvature of the wavefront at the fluxon root, the fluxon core structure can be analyzed in detail. Such analysis and its theoretical simulation are now in progress.

We here used a low T_c superconductor, Pb, to check the availability of our electron holographic method for research on superconductors. We are now carrying out the experiment on high-T_c superconductors, not only in the static, but also dynamical manner.

REFERENCES

1. Tonomura A. (1987) Applications of electron holography. Rev Mod Phys 59:639-669.
2. Huebener RP. (1979) Magnetic flux structures in superconductors. Springer-Verlag.
3. Gammel PL. Bishop DJ. Dolan Gj. Kwo JR. Murray CA. Schneemeyer LF. Waszczak JV. (1987) Observation of hexagonally correlated flux quanta in $YBa_2Cu_3O_7$. Phys Rev Lett 59: 2592-2595.
4. Hess HF. Robinson RB. Dynes RC. Valles JM. Waszczak JV. (1989) Scanning-tunneling-microscope observation of the Abrikosov flux lattice and the density of states near and inside a fluxoid. Phys Rev Lett 62: 214-216.
5. Matsuda T. Hasegawa S. Igarashi M. Kobayashi T. Naito M. Kajiyama H. Endo J. Osakabe N. Tonomura A. Aoki R. (1989) Magnetic field observation of a single flux quantum by electron-holographic interferometry. Phys Rev Lett 62: 2519-2522.
6. Aharonov Y. Bohm D. (1959) Significance of electromagnetic potentials in the quantum theory. Phys Rev 115: 485-491.
7. Kosterlitz JM. Thouless D. (1973) Ordering, metastability and phase transitions in two-dimensional systems. J Phys C6: 1181-1203.
8. Hasegawa S. Kawasaki T. Endo J. Tonomura A. Honda Y. Futamoto M. Yoshida K. Kugiya F. Koizumi M. (1989) Sensitivity-enhanced electron holography and its application to magnetic recording investigations. J Appl Phys 65: 2000-2003.

FIGURE CAPTIONS

Fig. 1. Experimental methods to observe magnetic flux structures in superconductors.
Fig. 2. Phase shift of electron wave caused by magnetic flux.
Fig. 3. Electron wavefront deformation in a holography electron microscope.
Fig. 4. Optical reconstruction system with fringe scanning interferometry.
Fig. 5. Interference micrographs directly showing magneic fluxons.
Fig. 6. Electron wavefront reconstructed from the hologram by fringe scanning interferometry.

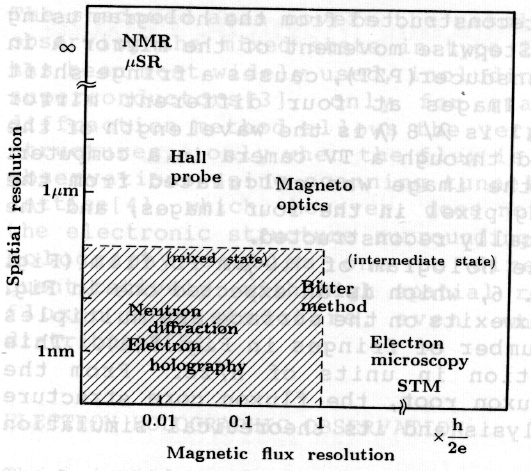

Fig. 1.

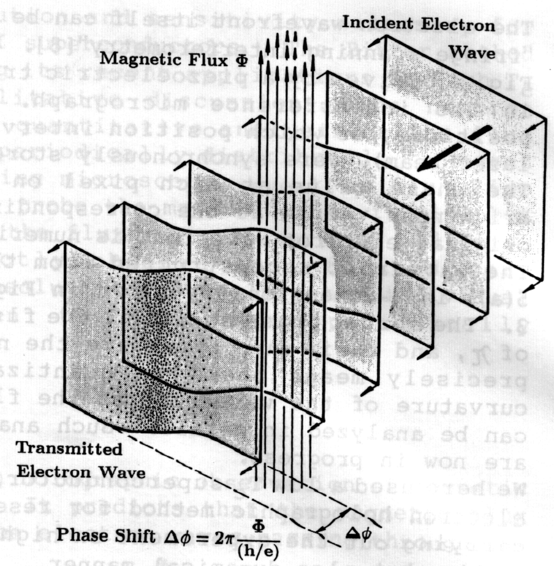

Fig. 2.

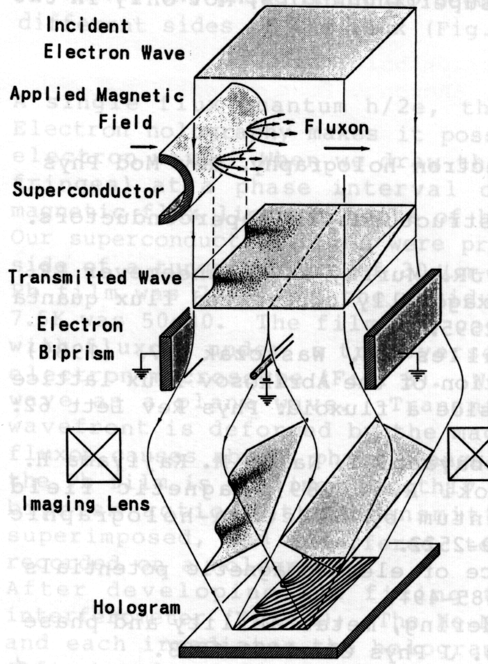

Fig. 3.

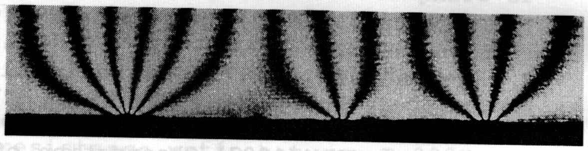

(a) Pb film of 1.0 μm thickness.

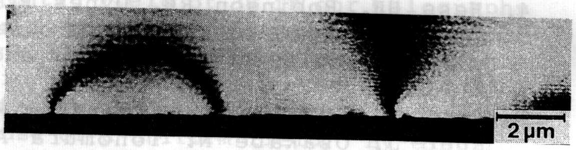

(b) Pb film of 0.2 μm thickness.

Fig. 5.

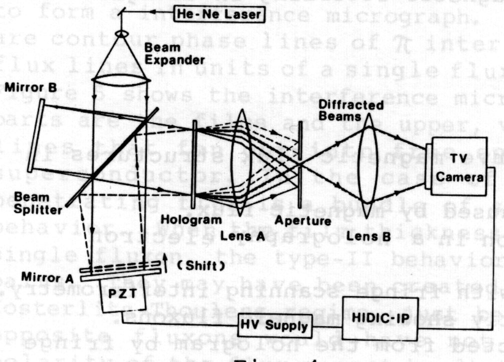

Fig. 4.

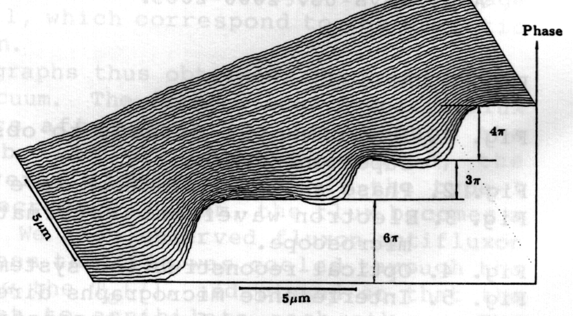

Fig. 6.